Discovery of Novel Aldose Reductase Inhibitors Using a Protein Structure-Based Approach: 3D-Database Search Followed by Design and Synthesis

Yoriko Iwata,[†] Mitsuhiro Arisawa,[‡] Ryuji Hamada,[‡] Yasuyuki Kita,[‡] Miho Y. Mizutani,[§] Nobuo Tomioka,[§] Akiko Itai,[§] and Shuichi Miyamoto*[,†]

Exploratory Chemistry Research Laboratories, Sankyo Co., Ltd., 1-2-58, Hiromachi, Shinagawa-ku, Tokyo 140-8710, Japan, Graduate School of Pharmaceutical Sciences, Osaka University, 1-6 Yamada-oka, Suita, Osaka 565-0871, Japan, and Institute of Medicinal Molecular Design, 5-24-5 Hongo, Bunkyo-ku, Tokyo 113-0033, Japan

Received November 13, 2000

Aldose reductase (AR) has been implicated in the etiology of diabetic complications. Due to the limited number of currently available drugs for the treatment of diabetic complications, we have carried out structure-based drug design and synthesis in an attempt to find new types of AR inhibitors. With the ADAM&EVE program, a three-dimensional database (ACD3D) was searched using the ligand binding site of the AR crystal structure. Out of 179 compounds selected through this search followed by visual inspection, 36 compounds were purchased and subjected to a biological assay. Ten compounds showed more than 40% inhibition of AR at a 15 μg/mL concentration. In a subsequent lead optimization, a series of analogues of the most active compound were synthesized based on the docking mode derived by ADAM&EVE. Many of these congeners exhibited higher activities compared to the mother compound. Indeed, the most potent, synthesized compound showed a ~20-fold increase in inhibitory activity (IC_{50} = 0.21 vs 4.3 μM). Furthermore, a hydrophobic subsite was newly inferred, which would be useful for the design of inhibitors with improved affinity for AR.

Introduction

The polyol pathway has been implicated in the etiology of secondary complications of diabetes.[1−3] Aldose reductase (AR) is the first enzyme of this pathway and is widely distributed in mammalian tissues.[4] In the presence of NADPH, the enzyme converts glucose to sorbitol, which is only slowly metabolized to fructose by sorbitol dehydrogenase, the other enzyme in the pathway. Aldose reductase inhibitors (ARIs) block the flux of glucose through the pathway and, in animal models of diabetes, prevent or reverse functional deficits and structural damage in the lens, retina, kidney, and peripheral nerves. A variety of structurally diverse compounds have been observed to inhibit AR. As can be seen in Chart 1, these compounds can be divided into two general classes of ARIs, those containing a carboxylic acid moiety and those having rigid spirohydantoins or related ring systems.[5−8] Although several of these compounds have progressed to the clinical level, only a few such drugs are currently on the market.

AR consists of a single polypeptide chain consisting of 315 residues. Several crystal structures of the enzyme have been solved by X-ray crystallography. It folds into a β/α barrel with a core of eight parallel β strands.[9] The ligand binding site is a large, deep, elliptical pocket with the nicotinamide ring of the NADPH cofactor at the base. Although a definite catalytic mechanism has not yet been determined, the crystal structures suggest the involvement of Tyr48 and Lys77 as well as the nicotinamide ring in the catalytic reaction.[10] A point mutation study[11] and a very recent computer simulation study[12] showed that Tyr48 acts as the proton donor in the reduction, and neutral His110 has a role in substrate binding during the catalysis although another computer modeling study[13] suggested that His110 was the proton donor. A potential anion binding site delineated by the nicotinamide ring, Tyr48, and His110 at the bottom of the cavity is suggested by the crystallographic and molecular modeling studies.[10,14]

In line with the current pace of X-ray crystallographic technologies as well as advances in the human genome project, structural determinations of macromolecules are increasing. Structure-based drug design (SBDD) has therefore become more and more important as a rational approach to the discovery of leads and their optimization.[15,16] It includes methods such as de novo design, 3D search, and docking studies and has been applied to the development of inhibitors, such as those of HIV protease and integrase.[17,18] Due to the limited number of currently available drugs for the treatment of diabetic complications, we applied the SBDD to ARIs in an attempt to find new types of leads.

In the pharmaceutical industry an acceptable lead typically has a dissociation constant of 10 μM or better.[19] Some successful results from a 3D search using the DOCK program have been summarized by Kuntz.[20] Typically, of the 100 to 200 best-scoring compounds, 10−50 were selected for biological testing and between 2 and 20% of the compounds tested showed inhibition in the micromolar range (5 to 900 μM). Very recently,

* To whom correspondence should be addressed: Exploratory Chemistry Research Laboratories, Sankyo Co., Ltd., 1-2-58, Hiromachi, Shinagawa-ku, Tokyo 140-8710, Japan. Tel: +81-3-3492-3131. Fax: +81-3-5436-8570. E-mail: miya@shina.sankyo.co.jp.
[†] Sankyo Co., Ltd.
[‡] Osaka University.
[§] Institute of Medicinal Molecular Design.

10.1021/jm000483h CCC: $20.00
Published on Web 04/27/2001

Chart 1. Chemical Structures of Known ARIs

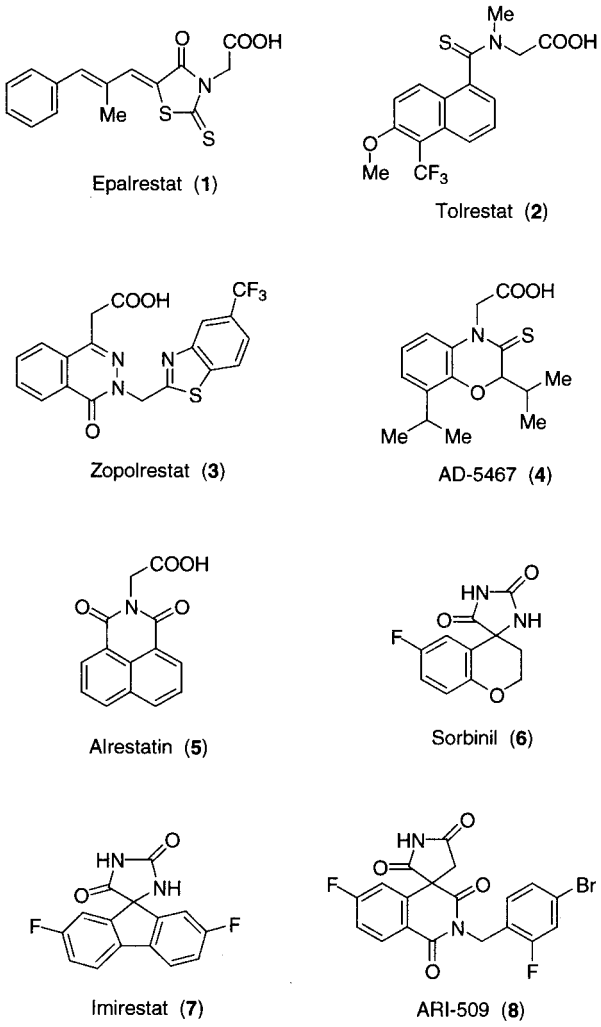

Zhang et al. carried out a 3D search to look for protein tyrosine phosphatase inhibitors.[21] From the 2000 compounds identified by DOCK, 25 were purchased for assay. Seven of them exhibited inhibition in the range between 21 and 510 μM. Pang et al. also reported on a virtual screening with the EUDOC program, identifying four farnesyltransferase inhibitors with IC_{50} values in the range of 25 to 100 μM.[22] Our 3D search results obtained by the ADAM&EVE program[23] are in no way inferior to these results.

Recently, Lee et al. presented a docking study in which some of the compounds shown in Chart 1 were extensively examined.[24] On the basis of the binding modes and inhibitory activities of those compounds, pharmacophore requirements for ARIs were discussed. Mura et al. reported on the design and synthesis of compounds based on a docking study of a known ARI.[25] With respect to the discovery by the 3D search, however, only a disappointing result has been briefly reported by Petrash et al. so far.[26] That is, among the approximately 30 highest scoring compounds derived by DOCK were several aromatic aldoximes that had inhibition constants in the micromolar range. Unfortunately, these were similar to known benzaldoximes with comparable inhibition constants.[27] As far as we know, therefore, the present study is the first successful example of the discovery of novel potent ARIs through a 3D-database search followed by design and synthesis.

Methods

Computational Chemistry. 1. Enzyme Structure. Although several X-ray crystal structures of AR have been registered in the Protein Data Bank (PDB),[28] no complex structures with potent inhibitors and with side chain atoms were available when our project started. The crystal structure of the ternary complex which includes cofactor NADPH and glucose-6-phosphate (G6P) was used in this study. Its code name in the PDB is 2acq, and the crystallographic resolution is 1.76 Å.[10] Since the crystal structure of bovine lens AR (used for the inhibition assays in this study) is not known, calculations were performed on human AR; however, the two sequences have ~90% homology, and residues constituting the binding site are highly conserved. The His, Asn, and Gln side chains were analyzed using the Guess_NOHQ program.[29] Some terminal conformations were flipped when they were built the wrong way around, and the suitable protonation forms of the imidazole ring were determined.

The oxidized form of NADPH ($NADP^+$), which is the crystal-bound form of the coenzyme,[10] was used in all calculations although several recent reports[30−32] indicated that inhibitor binding is equal to both the AR-NADPH and AR-$NADP^+$ complexes. With respect to the partial atomic charges of $NADP^+$, those in the AMBER database[33] were used for the adenine and ribose rings. As for each of the remaining nicotinamide and diphosphate moieties, a single-point ab initio calculation was carried out with a 6-31G* basis set using the Spartan program[34] to obtain the electrostatic potential charges.

In addition to the solvent water molecules, G6P was also removed from the crystal structure, and the resulting binary complex with $NADP^+$ was used for the calculation. Hydrogen atoms were added to the complex structure and geometry-optimized with the adopted-basis Newton Raphson (ABNR) algorithm[35] using the QUANTA/CHARMm system.[36]

2. 3D-Database Search. The rectangular region of 16 × 16 × 20 $Å^3$, including the catalytic and the G6P binding sites, was specified as the ligand binding site where docking of the compounds was evaluated. Using the in-house program CALGRID, the van der Waals interaction, electrostatic interaction, and hydrogen bonding energies were calculated at each grid point with a 0.4 Å interval within the region. On the basis of the grid data, the ADAM&EVE program searched the 3D database of the Available Chemicals Directory[37] (ACD3D) to identify what would fit into the ligand binding site. ACD3D consists of around 120 000 reagents whose 3D structures were constructed in-house from the ACD 2D database. Although only one conformation is registered for each entry of ACD3D, ADAM&EVE performed the systematic conformational search of the ligand at the time of docking.

After initial positioning of the ligand using two or three of the potential hydrogen bond sites distributed over the ligand binding pocket, the ADAM&EVE program optimizes the ligand conformation using the simplex method. The minimum number of hydrogen bonds formed in the optimized structure was set to 2. In addition, a hydrogen bond formation with one of the five atoms located in the bottom of the binding pocket was set as criteria. These atoms comprise the Oη of

Scheme 1. Synthesis of Substituted 2-Methyl-indole-3-acetic Acids (**19**−**32**)[a]

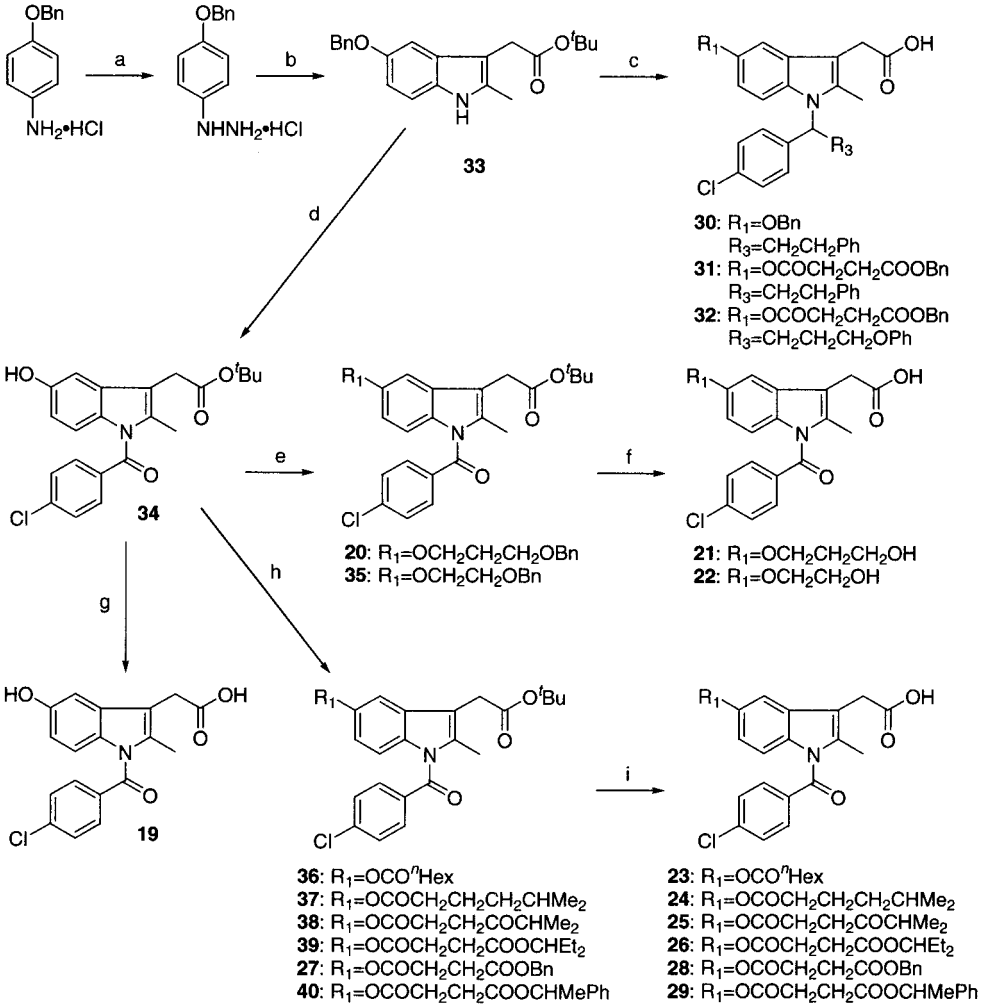

[a] Reagents and conditions: (a) (1) $NaNO_2$, cHCl, (2) $SnCl_2$, cHCl, (3) 1 N HCl−EtOH; (b) levulinic acid ^{t}buthyl ester, NaOAc, AcOH; (c) for **30**, (1) ^{t}BuOK, ^{p}$ClC_6H_4CBrCH_2CH_2Ph$, DMF, (2) CF_3COOH; for **31** and **32**, (1) ^{t}BuOK, ^{p}$ClC_6H_4CBrR_3$, DMF, (2) Pd/C, H_2, AcOEt−AcOH, (3) R_1CO_2H, DCC, DMAP, CH_2Cl_2, (4) neat, 180-190 °C or CF_3COOH; (d) (1) ^{t}BuOK, ^{p}ClC_6H_4COCl, THF, (2) Pd/C, H_2, AcOEt−AcOH; (e) R_1H, DEAD, PPh_3, THF; (f) for **21**, (1) CF_3COOH, (2) Pd/C, H_2, AcOEt−AcOH; for **22**, (1) Pd/C, H_2, AcOEt−AcOH, (2) CF_3COOH; (g) CF_3COOH; (h) R_1CO_2H, DCC, DMAP, CH_2Cl_2; (i) CF_3COOH (only for **28**, neat, 180−190 °C).

Tyr48, the Nϵ2 of His110, the Nϵ1 of Trp, and the Sγ of Cys298 as well as the nitrogen atom of the nicotinamide of $NADP^+$. The maximum energy (i.e., unfavorable limit) of the van der Waals interaction was set to −27 kcal/mol. Only compounds with a molecular weight of >250 and at least one ring structure were included.

Among the hit compounds identified using the above search criteria, further selection was performed based on the total interaction energy values as well as the visual inspection with computer graphics using the GREEN program.[38] In this examination, overall fit and how well the compound complemented the shape of the bottom of the binding site were taken into account, together with exclusions based upon considerations of chemical diversity and structural flexibility.

3. Design Based on the Active Compound. With respect to the most potent compound yielded by the 3D search, a rational design was performed with the QUANTA/CHARMm system starting from the docking mode derived by ADAM&EVE. First, the modified structures were built taking into account the van der Waals interactions and hydrogen bond formations. Second, the conformations of the modified moieties were manually changed to search for favorable interactions with the enzyme. Finally, the whole ligand structures were energy-minimized by the ABNR algorithm with the enzyme structure fixed. A distance-dependent dielectric constant of 4*r* was used in the CHARMm energy calculations.

Synthetic Chemistry. ^{t}Butyl 5-benzyloxy-2-methylindole-3-acetate (**33**) was prepared from commercially available 4-benzyloxyaniline hydrochloride using Fisher's indole synthesis (Scheme 1). N-Alkylated indoles (**30**−**32**) were synthesized via N-alkylation of **33** in the presence of ^{t}BuOK followed by chemical transformations. ^{t}Butyl 5-benzyloxy-1-(*p*-chlorobenzoyl)-2-methylindole-3-acetate (**34**) was prepared from **33** and *p*-chlorobenzoyl chloride in the presence of ^{t}BuOK. De-esterification of **34** gave 1-(*p*-chlorobenzoyl)-5-hydroxy-2-methyl-indole-3-acetic acid (**19**). Treatment of **34** with the corresponding alkyl halide, DEAD, and PPh_3 in THF afforded the O-alkylated compounds, **20** and **35**. Treatment of **20** and **35** with CF_3COOH led to the hydrolyzed compounds **21** and **22**, respectively. O-Acylated compounds, **36**, **37**, **38**, **39**, **27**, and **40** were prepared from **34** and the corresponding carboxylic acid in the presence of DCC and DMAP. Treatment of **36**−**39**, **27**, and **40**

Table 1. AR Inhibitory Activities and van der Waals Interaction Energies of Compounds **9**−**18**

compd	inhibition (%)[a] 5 (μg/mL)	inhibition (%)[a] 15 (μg/mL)	IC_{50} (μM)[a]	vdw energy[b] (kcal/mol)
9	49 (51)	70	18	−27.9
10	40	56 (47)		−31.5
11	68 (72)	83	5.0 (3.6)	−29.7
12	35 (56)	74 (70)	20 (14)	−28.9
13	36	50 (47)		−31.9
14	66 (72)	79 (72)	6.0 (4.6)	−29.9
15	47 (38)	74	9.8	−38.1
16	43 (42)	71	13	−32.7
17	38 (39)	63	18	−33.5
18		46 (36)		−30.4

[a] Values in parentheses are from a second independent experiment. [b] van der Waals interaction energy derived by the ADAM&EVE program.

with acid or heat gave the hydrolyzed compounds, **23**−**26**, and **28**−**29**, respectively.

Results and Discussion

3D-Database Search. The 3D database (ACD3D) was searched by the ADAM&EVE program to yield a total of 718 hits. Through visual inspection using computer graphics and total interaction energy values, 179 compounds were selected. From these, 36 compounds were purchased and subjected to AR inhibition assay. The 36 compounds were initially tested for their inhibition of AR at a concentration of 15 μg/mL. Ten out of the 36 compounds were classified as active. Their inhibition activities and chemical structures are shown in Table 1 and Chart 2, respectively. Seven of the compounds have a carboxyl group in their structures. Compound **16** has the same fused three-ring structure as alrestatin but lacks a carboxyl group. Interestingly, **11** is indomethacin, an antiinflammatory drug, and a similar indole-3-acetic acid ring structure was identified to have inhibitory activities against AR according to some of the patent literature. IC_{50} values were determined for the potent compounds and are listed in Table 1.

The IC_{50} values of the three most potent compounds, **11**, **14**, and **15**, are in the low micromolar range, that is, 4.3 (5.0 and 3.6), 5.3 (6.0 and 4.6), and 9.8 μM, respectively. Specifically, these figures appear to be superior to the micromolar range of inhibition constants observed for several aromatic aldoximes that were found by Petrash et al. through the 3D search of the Cambridge Structure Database against AR as mentioned above.[24] In general, our results presented here are among the top 3D-search studies currently in the literature. Although the potencies of our compounds were weaker than those of available drugs such as tolrestat (IC_{50} = 0.03−0.1 μM[6,14]), we believe that the main purpose of a 3D search is not to find compounds with ultrapotent activity. A realistic goal of a 3D search should be the discovery of new leads that can be subsequently used as the basis for further synthetic modifications as Wang et al. suggested.[39] In addition, the advantage of using the ADAM&EVE program is that a rational optimization can be pursued based on the binding mode obtained as shown in the following section.

It is well-known that docking scores exhibit poor correlation with real affinities.[19] Hol et al. reported little

Chart 2. Chemical Structures of ARIs Discovered in the 3D Search

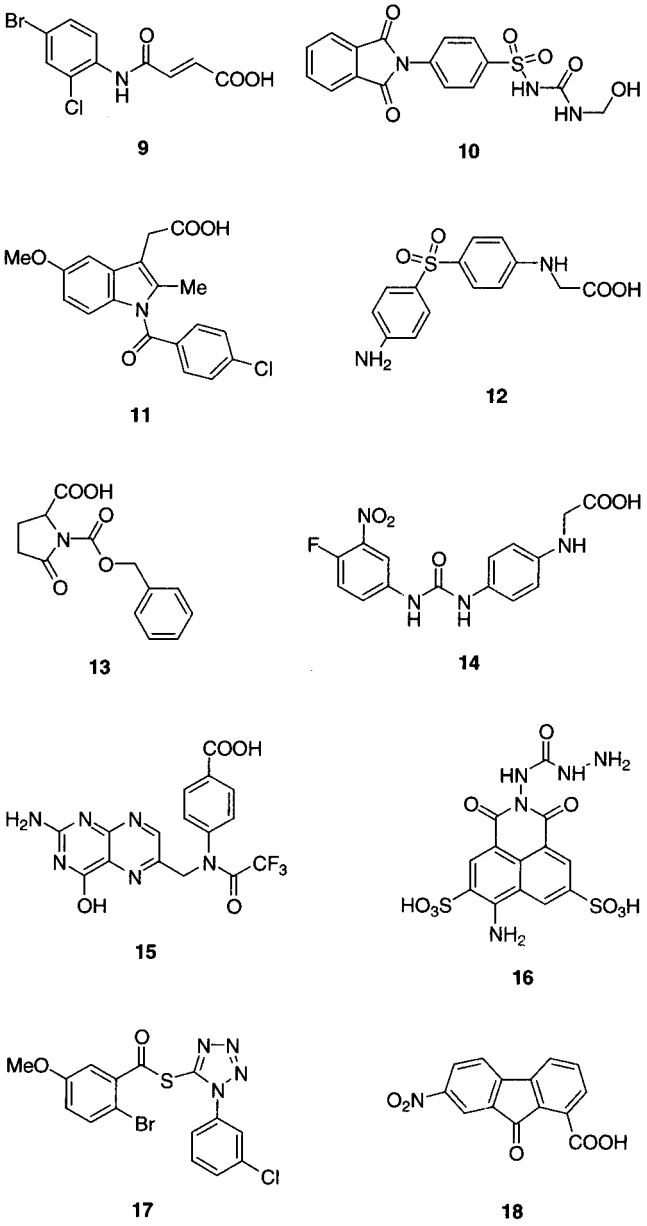

correlation between the docking scores and IC_{50} values in their 3D-search study.[40] Unfortunately, in our case as well, there appeared to be no correlation between the interaction energies derived by ADAM&EVE and the observed inhibitory potencies (Table 1). Scoring or energy evaluation is an important and challenging issue in SBDD.[41] Improvement of the interaction energy evaluation of ADAM&EVE is currently in progress, and preliminary calculations on another protein·ligand system have provided promising results.

The binding modes derived by ADAM&EVE are shown in Figure 1 for the three most potent compounds, **11**, **14**, and **15**. They fit into the middle of the long binding pocket, with good steric complementarity between the ligand and the bottom of the cavity. Hydrogen bonds with the Oη of Tyr48 and the Nϵ2 of His110 in the anion binding site were formed for **11** and **14**. The ureido group of **14** was hydrogen bonded to the Nϵ1 of Trp20 located in the mouth of the cavity. Compound **15** formed hydrogen bonds with the side chain of Cys298

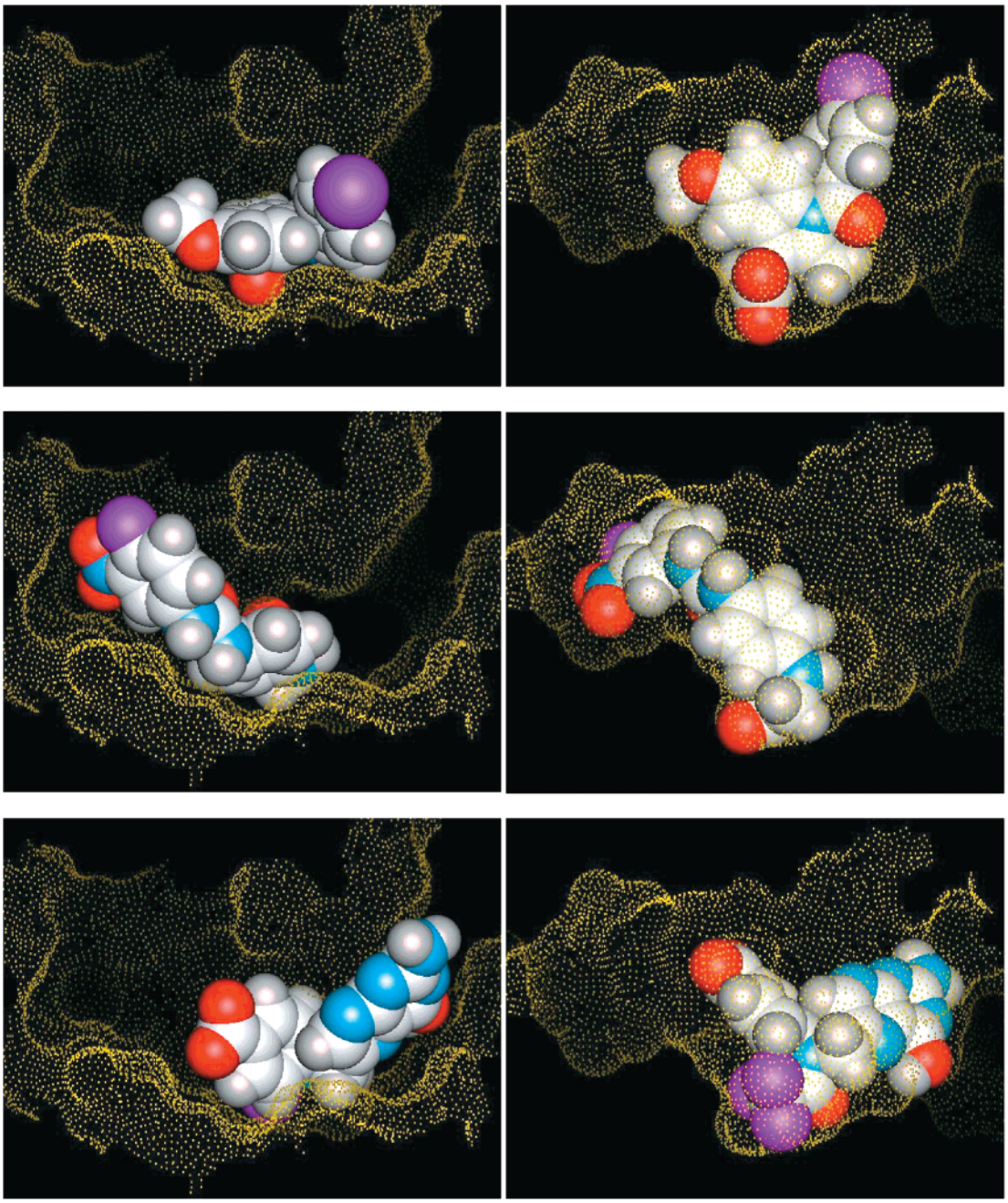

Figure 1. Complex structure models of AR and **11** (top), **14** (middle), and **15** (bottom). Top view of the large active site (left) and side view (right). The ligand binding site is represented by the Connolly surface in yellow. The inhibitors are rendered in CPK form, in which carbon and hydrogen are shown in white, oxygen in red, halogen in purple, and nitrogen in blue.

and the main chains of Ala299 and Leu300. It should be noted that the side chain of His110 was flipped based on our analysis. Judging from the docking structures, it appears that **11** and **14** would not have a favorable interaction with His110 in the original conformation registered in the PDB.

Interestingly, the carboxyl group of **15** was not situated at the bottom of the pocket but faced the solvent. Using the QUANTA/CHARMm system, a model was built with the docked orientation of the carboxylic group in the anion binding site. The interaction energy of the compound in the former orientation was calculated to be slightly lower than that in the latter, which was consistent with the orientation selected by ADAM&EVE. Geometry optimization of **11** using the CHARMm force field brought slight positional and torsional changes of the carboxyl moiety. In this complex structure, the carboxylate was electrostatically attracted to the positive nicotinamide ring of $NADP^+$. In addition, it was held in place with the same three hydrogen bonds to the Tyr48 hydroxyl, the Nϵ2 of His110, and the Nϵ1 of Trp111 (Figure 2) as those observed in the complex crystal structure of tolrestat.[42] The indole ring lay between the side chains of Trp20, Val47, and Phe122, and it was close to those of Trp79 and Trp219 with favorable van der Waals interactions. Although the carboxyl group of **14** was situated in the anion binding site, it was, if anything, positioned opposite to Trp20 rather than Trp111. Compound **16** also has the same fused three-ring system as alrestatin but its sulfonyl groups are substituted in different positions compared with the carboxyl group of alrestatin. The sulfonyl

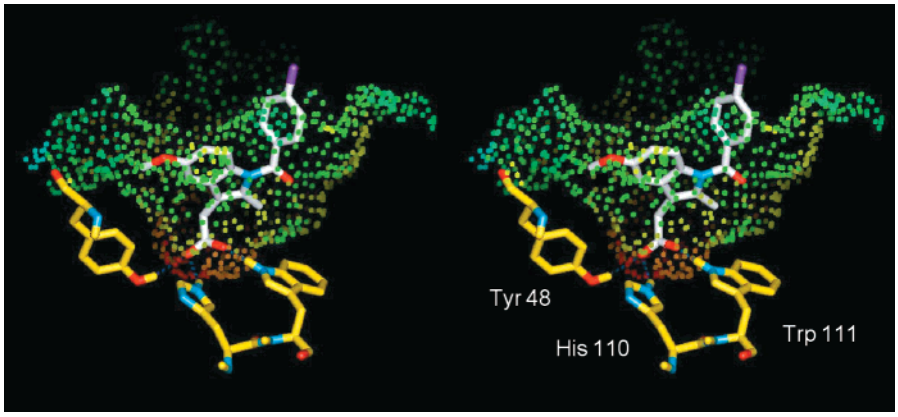

Figure 2. Stereoview of the complex structure model of AR (yellow) and **11** (white) in stick form. Connolly surface of the enzyme is colored by the electrostatic potential (positive, red; neutral, green; negative, blue) calculated using the QUANTA/CHARMm system. Hydrogen bonds with Tyr48, His110, and Trp111 are drawn as dashed lines. Nonpolar hydrogens are omitted for clarity.

Table 2. AR Inhibitory Activities of Compound **11** and Its Analogues

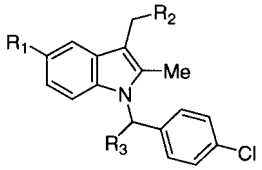

compd	R_1	R_2	R_3	IC_{50} (μM) [a]
11	OMe	COOH	=O	~4.3
19	OH	COOH	=O	3.2
20	$OCH_2CH_2CH_2OCH_2Ph$	COO^tBu	=O	*b*
21	$OCH_2CH_2CH_2OH$	COOH	=O	4.2
22	OCH_2CH_2OH	COOH	=O	3.4
23	OCO-*n*-Hex	COOH	=O	2.9
24	$OCOCH_2CH_2CH_2CH(Me)_2$	COOH	=O	1.9
25	$OCOCH_2CH_2COCH(Me)_2$	COOH	=O	1.4
26	$OCOCH_2CH_2COOCH(Et)_2$	COOH	=O	0.54
27	$OCOCH_2CH_2COOCH_2Ph$	COO^tBu	=O	*b*
28	$OCOCH_2CH_2COOCH_2Ph$	COOH	=O	0.21
29	$OCOCH_2CH_2COOCH(Me)Ph$	COOH	=O	0.31
30	OCH_2Ph	COOH	CH_2CH_2Ph	9% (9.5 μM)
31	$OCOCH_2CH_2COOCH_2Ph$	COOH	CH_2CH_2Ph	10% (8.0 μM)
32	$OCOCH_2CH_2COOCH_2Ph$	COOH	$CH_2CH_2CH_2OPh$	17% (7.6 μM)

[a] IC_{50} or percent inhibition (at a given micromolar concentration). [b] No inhibition was observed at a concentration of 5 μg/mL.

moiety without the *o*-amino substituent was located in the anion binding site and the other sulfonyl group, at the surface of the complex.

Lead Optimization. The most potent compound was selected as the lead, on which we then carried out structure modifications. The docking mode derived by ADAM&EVE (Figures 1 and 2) revealed that the molecule did not fully occupy the long binding cavity. It was also found that no hydrogen bond was formed between the ligand and enzyme residues at the mouth of the pocket. In designing the modified ligands, therefore, we took into account the possibility of hydrogen bonds with the side chain of Trp20 and the main chains of Lys21, Val47, Tyr48, Ala299, and Leu300. In addition, the hydrophobic interactions with the side chains of Lys21, Val47, Pro23, Pro24, Phe122, Trp219, and Leu301 were considered. The designed models were initially constructed using the QUANTA/CHARMm system. After geometry optimization of the modeled ligands by molecular mechanics calculations, those staying at the binding pocket as expected were selected as synthetic candidates.

Table 2 includes the chemical structures of the synthetic analogues of **11** and their inhibitory activities against AR. These compounds were initially tested for their inhibition at a concentration of 5 μg/mL. Compounds **20** and **27** with the protected carboxyl group lost their inhibitory activities. This seemed to support the ADAM&EVE-derived docking mode where the carboxyl group fit into the anion binding site. The significant decreases in the inhibitory activities of **30**−**32** indicated that the structural modifications of R_3 were unsuitable. The substituents of R_3 were assumed to approach Phe122 and Ala299-Leu301. It was revealed that the loop Phe121-Thr135 and the short segment Cys298-Cys303 were liable to incur conformational changes based on the molecular dynamics simulation[13] of AR and the complex crystal structure with zopolrestat,[43] whose coordinates are as yet not available. These substituents of R_3 may cause unfavorable conformational changes in this part of the enzyme.

Other analogues of **11** in Table 2 exhibited similar or higher potencies compared to the lead compound **11**. No gain in activity was observed for **21** or **22**. The reason for this might be that a hydrogen bond could not be effectively formed with the terminal hydroxy group of R_1 or that they lack an ester carbonyl in the stem of R_1. The compounds with a branched alkyl group in R_1

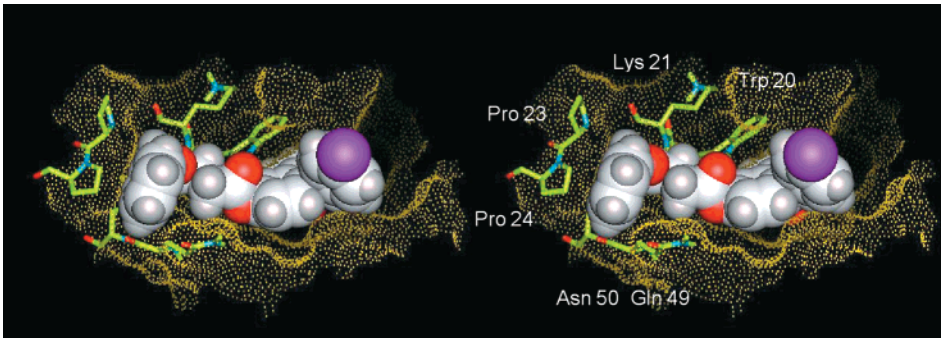

Figure 3. Stereoview of the complex structure model of AR (green-yellow) and **28** (white). Connolly surface of the enzyme is shown in yellow. Selected residues of AR are represented in stick form. Nonpolar hydrogen atoms of these residues are omitted for clarity. Compound **28** is rendered in CPK form, in which carbon and hydrogen are shown in white, oxygen in red, chlorine in purple, and nitrogen in blue.

showed relatively potent inhibitory activities. Those with a terminal ester group in R_1 exhibited rather potent activities. Indeed, the IC_{50} value of **28** was 0.21 μM, indicating the achievement of an around 20-fold increase in the activity compared to the mother compound.

Figure 3 illustrates the complex model of **28** and AR. In this docked conformation, the ester carbonyl oxygen of the root of R_1 was hydrogen bonded with the Hϵ1 of the side chain of Trp20. The terminal phenyl group fit into the hydrophobic pocket comprising the methylene group of the side chains of Pro23, Pro24, Gln49, and Asn50. Alternatively, it could be accommodated in the neighboring hydrophobic cavity consisting of the side chains of Lys21 and Pro23. In this complex model, the terminal ester moiety was not involved in the hydrogen bonding but was considered to contribute to the van der Waals interaction for the sake of good steric complementarity between the ligand carbonyl group and the enzyme.

The IC_{50} value of 0.31 μM for **29** was slightly larger than that of 0.21 μM for **28**. Compound **29** was a racemic mixture, and one of the isomers was calculated to fit better into the hydrophobic pocket than the other. It was therefore presumed that the inhibitory activity of a suitable isomer of **29** would be comparable to that of **28**. With respect to the potent compounds, **26**, **28**, and **29**, the terminal hydrophobic part of R_1 was considered to interact with the alkyl moiety of the side chains of Lys21, Pro23, Pro24, Gln49, and/or Asn50. This hydrophobic subsite of AR was not occupied in the binding of zopolrestat or tolrestat as was observed in their complex crystal structures. This newly discovered subsite would be useful for the design of potent ARIs although experimental verification such as by mutation studies is necessary to establish that the hydrophobic subsite is indeed an important pharmacophore.

The potency of the most effective compound **28** (IC_{50} = 0.21 μM) is superior to that of sorbinil and recently reported isoxazolopyridazinones (IC_{50} = 3 and ~5 μM, respectively[44]) but inferior to that of epalrestat (IC_{50} = 0.01 μM[8]) and tolrestat (IC_{50} = 0.03−0.1 μM[6,14]). The IC_{50} value of 0.21 μM for **28** is comparable to that of the 0.15 μM that was successfully attained by Mura et al. through the design and synthesis based on the docking study of a known ARI.[25] Their compound is, however, a composite of the known tricyclic pyridazinone skeleton and the benzothiazole ring of zopolrestat. On the contrary, **28** was discovered by the 3D-database search followed by the design and synthesis of a novel substituent, providing new insight into the interaction between AR and ARI. Further improvement of potency and the selectivity evaluation with respect to other related enzymes are subjects for investigation in the future.

Conclusion

The present study is the first successful example of the discovery of novel potent inhibitors of AR through a 3D-database search followed by design and synthesis. Using the ADAM&EVE program, the ACD3D database was searched based on the ligand binding site of the crystal structure of AR. This search led to the identification of 10 inhibitors with significant inhibitory activities at a concentration of 15 μg/mL. The potent inhibitions exhibited by around 30% of the compounds subjected to inhibition assay illustrate the power of the ADAM&EVE approach for the discovery of new types of leads. Furthermore, a ~20-fold increase in inhibitory activity was achieved by subsequent design and synthesis based on the complex structure model derived by docking. Our results demonstrate the effectiveness of SBDD for the discovery of leads and the ensuing optimization. In addition, the hydrophobic subsite inferred from the complex structure models of the most potent compounds would be useful for the design of new ARIs with improved potency.

Experimental Section

Synthetic Chemistry. All compounds were fully characterized (^{1}H, IR, mass). IR spectra (cm^{-1}) were recorded using a KBr pellet. ^{1}H NMR spectra were recorded in $CDCl_3$, unless otherwise mentioned, at 200, 270, 300, or 500 MHz with TMS as an internal standard. E. Merck silica gel 60 for column chromatography and E. Merck precoated TLC plates, silica gel F_{254}, for preparative thin-layer chromatography were used. The organic layers were dried over anhydrous $MgSO_4$ or Na_2SO_4.

^{t}Butyl 5-Benzyloxy-2-methyl Indole 3-Acetate (33). To a solution of 4-benzyloxy aniline hydrochloride (2.11 g, 8.94 mmol) in concentrated HCl (15.0 mL) was added a solution of sodium nitrate (617 mg, 8.94 mmol) in H_2O (2.25 mL) dropwise at 0 °C, and the mixture was stirred for 25 min. To the mixture was added $SnCl_2$ (4.75 g. 25.0 mmol) dropwise at −25 °C. The mixture was stirred for 4 h and then filtered, and the residue was washed with concentrated HCl. The obtained solid was then dissolved in 25% KOH and Et_2O, and the organic compound was extracted with Et_2O, dried over Na_2SO_4, and filtered. The organic layer was partially concentrated under

reduced pressure and filtered to get crystals. To these crystals was added 1 N HCl−EtOH (10.0 mL), and the solvent was removed to give 4-benzyloxyphenylhydrazine hydrochloride (897 mg, 40%) as dark yellow plates. To a stirring solution of the obtained compound (897 mg, 3.58 mmol) in acetic acid (10.0 mL) was added sodium acetate (295 mg, 3.58 mmol) at room temperature. The mixture was refluxed for 2 h and then neutralized with aqueous NaOH, and the organic compound was extracted with Et_2O, dried over Na_2SO_4, and concentrated in a vacuum. The crude residue was subjected to column chromatography (*n*-hexane:AcOEt = 6:1∼4:1) to give **33** (783 mg, 62%) as a dark yellow plate: ^{1}H NMR (300 MHz, $CDCl_3$) δ (ppm) 7.49 (1H, s), 7.46−7.28 (5H, m), 7.14 (1H, d, J = 9.0 Hz), 7.10 (1H, d, J = 2.4 Hz), 6.84 (1H, dd, J = 9.0 Hz, 2.4 Hz), 5.10 (2H, s), 3.54 (2H, s), 2.38 (3H, s), 1.42 (9H, s); IR(KBr) 3403, 1720 cm^{-1}; LRMS (EI) *m*/*z* 351 (M^+). HRMS (EI) calcd for $C_{22}H_{25}NO_3$, 351.1834; found, 351.1837.

^{t}Butyl 5-Benzyloxy-1-(4-chlorobenzoyl)-2-methyl Indole 3-Acetate (34). To a solution of **33** (600 mg, 1.71 mmol) in THF (28.0 mL) was added ^{t}BuOK (229 mg, 2.05 mmol), and the mixture was stirred for 20 min. To the mixture was added 4-chlorobenzoyl chloride (0.260 mL, 2.05 mmol), and it was then stirred for 11 h. The reaction was quenched with saturated aqueous NH_4Cl. The organic compound was extracted with AcOEt, washed with brine, dried over Na_2SO_4, filtered, and concentrated. The crude residue was subjected to column chromatography (*n*-hexane:AcOEt = 4:1∼2:1) to give a 5-benzyloxy derivative (844 mg, 100%) as dark orange crystals. To the stirring solution of the derivative (1.10 g, 2.24 mmol) in AcOEt (22.0 mL) and AcOH (20.0 mL) was added Pd/C (110 mg) under H_2 (3.8 atm). The mixture was stirred for 3 h and then filtered, and the crude residue was subjected to column chromatography (*n*-hexane:AcOEt = 3:1) to give **34** (774 mg, 87%) as a pale yellow powder: ^{1}H NMR (300 MHz, $CDCl_3$) δ (ppm) 7.65 (2H, d, J = 8.6 Hz), 7.46 (2H, d, J = 8.6 Hz), 6.91 (1H, d, J = 2.4 Hz), 6.84 (1H, d, J = 8.8 Hz), 6.52 (1H, dd, J = 8.8 Hz, 2.4 Hz), 3.54 (2H, s), 2.35 (3H, s), 1.45 (9H, s); LRMS (EI) *m*/*z* 399 (M^+). HRMS (EI) calcd for $C_{22}H_{22}NO_4Cl$, 399.1237; found, 399.1229.

1-(4-Chlorobenzyl)-5-hydroxy-2-methyl Indole 3-Acetic Acid (19). Compound **34** (201 mg, 0.503 mmol) was dissolved in CF_3COOH (7.00 mL), and the mixture was stirred for 1 h. The solvent was removed, and the crude residue was recrystallized (from CH_2Cl_2) to give **19** (152 mg, 88%) as white crystals: ^{1}H NMR (200 MHz, $CDCl_3$) δ (ppm) 7.67 (2H, d, J = 8.7 Hz), 7.47 (2H, d, J = 8.7 Hz), 6.89 (1H, d, J = 2.2 Hz), 6.81 (1H, d, J = 8.8 Hz), 6.79 (1H, dd, J = 8.8 Hz, 2.2 Hz), 3.62 (2H, s), 2.37 (3H, s); LRMS (EI) *m*/*z* 343 (M^+). HRMS (EI) calcd for $C_{18}H_{14}NO_4Cl$, 343.0611; found, 343.0615.

^{t}Butyl 5-(3-Benzyloxypropoxy)-1-(4-chlorobenzoyl)-2-methyl Indole 3-Acetate (20). To a solution of **34** (84.9 mg, 0.212 mmol) in THF (3.00 mL) was added dropwise a mixture of 3-benzyloxypropanol (61.0 mg, 0.193 mmol), PPh_3 (105 mg, 0.212 mmol), and DEAD (40% solution in toluene, 0.0950 mL, 0.212 mmol) at 0 °C, and the mixture was stirred at the same temperature for 10 min. The mixture was then stirred at room temperature for 2 days. To the mixture was added H_2O, and the organic compound was extracted with AcOEt, washed with brine, dried over Na_2SO_4, filtered, and concentrated. The crude residue was subjected to column chromatography (*n*-hexane:AcOEt = 3:1) to give **20** (58.0 mg, 50%) as a colorless amorphous solid: ^{1}H NMR (200 MHz, $CDCl_3$) δ (ppm) 7.66 (2H, d, J = 8.4 Hz), 7.46 (2H, d, J = 8.4 Hz), 7.34−7.29 (5H, m), 6.97 (1H, d, J = 2.4 Hz), 6.88 (1H, d, J = 9.8 Hz), 6.65 (1H, dd, J = 9.8 Hz, 2.4 Hz), 4.53 (2H, s), 4.11 (2H, t, J = 6.2 Hz), 3.68 (2H, d, J = 6.2 Hz), 3.55 (2H, s), 2.37 (3H, s), 1.44 (9H, s).

1-(4-Chlorobenzyl)-5-(3-hydroxypropoxy)-2-methyl Indole 3-Acetic Acid (21). Compound **20** (100 mg, 0.182 mmol) was dissolved in CF_3COOH (5.00 mL), and the mixture was stirred for 1.5 h. The solvent was removed, and the crude residue was subjected to preparative TLC (AcOEt) to give 5-(3-benzyloxypropoxy)-1-(4-chlorobenzoyl)-2-methyl indole 3-acetic acid (90.0 mg, 100%) as a colorless amorphous solid. To a solution of the obtained compound (90.0 mg, 0.182 mmol) in AcOEt (15.0 mL) and AcOH (5.00 mL) was added Pd/C (23.0 mg) under H_2 (3.8 atm), and the mixture was stirred for 12 h. The mixture was filtered, and the solvent was removed. The crude residue was subjected to column chromatography (CH_2Cl_2:MeOH = 10:1) to give **21** (51.2 mg, 70%) as a colorless amorphous solid: ^{1}H NMR (270 MHz, CD_3OD) δ (ppm) 7.67 (2H, d, J = 8.6 Hz), 7.53 (2H, d, J = 8.6 Hz), 7.04 (1H, s), 6.91 (1H, d, J = 8.9 Hz), 6.64 (1H, d, J = 8.9 Hz), 4.07 (2H, t, J = 6.1 Hz), 3.73 (2H, t, J = 6.3 Hz), 3.55 (2H, s), 2.26 (3H, s), 1.98−1.93 (2H, m); IR(KBr) 3450, 1685, 1612 cm^{-1}; LRMS (EI) *m*/*z* 401 (M^+). HRMS (EI) calcd for $C_{21}H_{20}NO_5Cl$, 401.1030; found, 401.1023.

1-(4-Chlorobenzyl)-5-(2-hydroxyethoxy)-2-methyl Indole 3-Acetic Acid (22). To a solution of **34** (223 mg, 0.656 mmol) in THF (9.00 mL) was added dropwise a mixture of 2-benzyloxyethanol (78.0 mg, 0.597 mmol), PPh_3 (147 mg, 0.656 mmol), and DEAD (40% solution in toluene, 0.240 mL, 0.656 mmol) at 0 °C, and the mixture was stirred at the same temperature for 10 min. The mixture was then stirred at room temperature for 18 h. To the mixture was added H_2O, and then organic compound was extracted with AcOEt, washed with brine, dried over Na_2SO_4, filtered, and concentrated. The crude residue was subjected to column chromatography (*n*-hexane:AcOEt = 5:1) to give ^{t}butyl 5-(2-benzyloxyethoxy)-1-(4-chlorobenzoyl)-2-methyl indole 3-acetate (58.0 mg, 50%) as a yellow oil. To a solution of the resulting compound (144 mg, 0.270 mmol) in AcOEt (8.00 mL) and AcOH (8.00 mL) was added Pd/C (36.0 mg) under H_2 (3.8 atm), and the mixture was stirred for 6.5 h. The mixture was filtered, and the solvent was removed. The crude residue was subjected to column chromatography (*n*-hexane:AcOEt = 3:1∼2:1) to give ^{t}butyl 1-(4-chlorobenzyl)-5-(2-hydroxyethoxy)-2-methyl indole 3-acetate (68.0 mg, 57%) as a pale yellow oil. This (57.0 mg, 0.128 mmol) was dissolved in CF_3COOH (2.00 mL) and stirred for 4 h. The solvent was removed, and the crude residue was subjected to preparative TLC (CH_2Cl_2:MeOH = 10:1) to give **22** (7.00 mg, 14%) as a colorless amorphous solid: ^{1}H NMR (300 MHz, CD_3OD) δ (ppm) 7.67 (2H, d, J = 8.7 Hz), 7.54 (2H, d, J = 8.7 Hz), 7.03 (1H, s), 6.90 (1H, d, J = 9.2 Hz), 6.70 (1H, d, J = 9.2 Hz), 4.05 (2H, t, J = 4.4 Hz), 3.86 (2H, t, J = 4.4 Hz), 3.71 (2H, s), 2.30 (3H, s); IR(KBr) 2920, 1684 cm^{-1}; LRMS (EI) *m*/*z* 387 (M^+). HRMS (EI) calcd for $C_{20}H_{18}NO_5Cl$, 387.0873; found, 387.0857.

General Procedure for 23−27 and 29. To a solution of **34** (0.100 mmol) in CH_2Cl_2 (1.50 mL) was added DCC (1.50 equiv), DMAP (0.100 equiv), and the corresponding acid (1.10 equiv), and the mixture was stirred for 12 h. The mixture was filtered, washed with H_2O and brine, dried over Na_2SO_4, filtered, and concentrated. The crude residue was subjected to column chromatography (*n*-hexane:AcOEt) to give O-acylated ^{t}butyl acetate. To a stirring solution of O-acylated ^{t}butyl acetate in CH_2Cl_2 (1.50 mL) was added CF_3COOH (0.400 mL), and the mixture was stirred for 1.5 h. The solvent was removed, and the crude residue was subjected to preparative TLC to give O-acylated acetic acid.

1-(4-Chlorobenzyl)-5-^{n}heptanoyloxy-2-methyl Indole 3-Acetic Acid (23). A pale yellow oil of 29% yield from **34**: ^{1}H NMR (300 MHz, $CDCl_3$) δ (ppm) 7.59 (2H, d, J = 8.4 Hz), 7.40 (2H, d, J = 8.4 Hz), 7.12 (1H, s), 6.88 (1H, d, J = 9.0 Hz), 6.68 (1H, d, J = 9.0 Hz), 3.59 (2H, s), 2.47 (2H, t, J = 7.5 Hz), 2.29 (3H, s), 1.67 (2H, t, J = 7.2 Hz), 1.35−1.25 (6H, m), 0.83−0.81 (3H, m); LRMS (EI) *m*/*z* 455 (M^+). HRMS (EI) calcd for $C_{25}H_{26}NO_5Cl$, 455.1499; found, 455.1494.

1-(4-Chlorobenzyl)-5-^{i}heptanoyloxy-2-methyl Indole 3-Acetic Acid (24). A yellow oil of 43% yield from **34**: ^{1}H NMR (300 MHz, $CDCl_3$) δ (ppm) 7.67 (2H, d, J = 8.3 Hz), 7.48 (2H, d, J = 8.3 Hz), 7.21 (1H, d, J = 2.1 Hz), 6.95 (1H, d, J = 8.7 Hz), 6.77 (1H, dd, J = 8.7 Hz, 2.1 Hz), 3.69 (2H, s), 2.54 (2H, t, J = 7.7 Hz), 2.39 (3H, s), 1.81−1.26 (5H, m), 0.91 (6H, d, J = 6.3 Hz); IR(KBr) 2957, 1755, 1713, 1693 cm^{-1}; LRMS (EI) *m*/*z* 455 (M^+). HRMS (EI) calcd for $C_{25}H_{26}NO_5Cl$, 455.1499; found, 455.1502.

Succinic Acid 1-Methylethyl Ester 3-Carboxymethyl-1-(4-chlorobenzoyl)-2-methyl Indol-5-yl Ester (25). A yellow oil of 48% yield from **34**: ^{1}H NMR (300 MHz, $CDCl_3$) δ (ppm) 7.66 (2H, d, J = 8.6 Hz), 7.47 (2H, d, J = 8.6 Hz), 7.21 (1H, d, J = 2.1 Hz), 6.94 (1H, d, J = 9.0 Hz), 6.77 (1H, dd, J = 9.0 Hz, 2.1 Hz), 3.67 (2H, s), 2.90−2.61 (5H, m), 2.37 (3H, s), 1.13 (6H, d, J = 6.9 Hz); LRMS (EI) m/z 492 (M^+ + Na). HRMS (EI) calcd for $C_{25}H_{24}NO_6ClNa$, 492.1190; found, 492.1186.

Succinic Acid 1-Ethylpropyl Ester 3-Carboxymethyl-1-(4-chlorobenzoyl)-2-methyl Indol-5-yl Ester (26). A yellow oil of 37% yield from **34**: ^{1}H NMR (300 MHz, $CDCl_3$) δ (ppm) 7.66 (2H, d, J = 8.4 Hz), 7.47 (2H, d, J = 8.4 Hz), 7.21 (1H, d, J = 1.8 Hz), 6.95 (1H, d, J = 9.0 Hz), 6.78 (1H, dd, J = 9.0 Hz, 1.8 Hz), 4.84−4.76 (1H, m), 3.67 (2H, s), 2.88 (2H, t, J = 6.5 Hz), 2.74 (2H, t, J = 6.6 Hz), 2.37 (3H, s), 1.62−1.52 (4H, m), 0.87 (6H, d, J = 7.5 Hz); IR(KBr) 2971, 1761, 1732, 1693 cm^{-1}; LRMS (FAB) m/z 536 (M^+ + Na); HRMS (FAB) calcd for $C_{27}H_{28}NO_7ClNa$, 536.1452; found, 536.1450.

Succinic Acid Benzyl Ester 3-^{t}Butoxycarboxymethyl-1-(4-chlorobenzoyl)-2-methyl Indol-5-yl Ester (27). A light brown amorphous solid of 99% yield from **34**: ^{1}H NMR (300 MHz, $CDCl_3$) δ (ppm) 7.57 (2H, d, J = 8.4 Hz), 7.38 (2H, d, J = 8.4 Hz), 7.30−7.21 (5H, m), 7.15 (1H, s), 6.88 (1H, d, J = 8.8 Hz), 6.64 (1H, d, J = 8.8 Hz), 5.07 (2H, s), 3.47 (2H, s), 2.87−2.65 (4H, m), 2.28 (3H, s), 1.35 (9H, s); LRMS (FAB) m/z 612 (M^+ + Na). HRMS (FAB) calcd for $C_{33}H_{32}NO_7ClNa$, 612.1765; found, 612.1778.

Succinic Acid 1-Phenylethyl Ester 3-Carboxymethyl-1-(4-chlorobenzoyl)-2-methyl-indol-5-yl Ester (29). A colorless oil of 40% yield from **34**: ^{1}H NMR (300 MHz, $CDCl_3$) δ (ppm) 7.60 (2H, d, J = 8.6 Hz), 7.41 (2H, d, J = 8.6 Hz), 7.27−7.12 (5H, m), 7.12 (1H, s), 6.85 (1H, d, J = 9.0 Hz), 6.63 (1H, d, J = 9.0 Hz), 5.85 (1H, q, J = 6.9 Hz), 3.60 (2H, s), 2.83−2.66 (4H, m), 2.30 (3H, s), 1.47 (3H, d, J = 6.9 Hz); IR(KBr) 2930, 1750, 1732, 1715, 1694 cm^{-1}; LRMS (FAB) m/z 570 (M^+ + Na). HRMS (FAB) calcd for $C_{30}H_{26}NO_7ClNa$, 570.1296; found, 570.1324.

Succinic Acid Benzyl Ester 3-Carboxymethyl-1-(4-chlorobenzoyl)-2-methyl-indol-5-yl Ester (28). Compound **27** (284 mg, 0.481 mmol) and Celite 535 (56.0 mg) were stirred at 190 °C for 30 min. The crude residue was subjected to column chromatography (CH_2Cl_2:MeOH = 15:1) to give **28** (101 mg, 39%) as a brown amorphous solid: ^{1}H NMR (300 MHz, $CDCl_3$) δ (ppm) 7.55 (2H, d, J = 8.4 Hz), 7.37 (2H, d, J = 8.4 Hz), 7.29−7.18 (5H, m), 7.11 (1H, d, J = 1.5 Hz), 6.84 (1H, d, J = 8.8 Hz), 6.64 (1H, dd, J = 8.8 Hz, 1.5 Hz), 5.05 (2H, s), 3.52 (2H, s), 2.77−2.65 (4H, m), 2.23 (3H, s).

5-Benzyloxy-1-[1-(4-chlorophenyl)-3-phenyl-propyl]-2-methyl Indole 3-Acetic Acid (30). To a solution of **33** (400 mg, 1.14 mmol) and ^{t}BuOK (154 mg, 1.37 mmol) in DMF (7.00 mL) was added a solution of p-$ClC_6H_4CHBrCH_2CH_2Ph$ in DMF (1.00 mL), and the mixture was stirred at room temperature for 14 h. To the mixture was added H_2O. The organic compound was extracted with AcOEt, washed with brine, dried over Na_2SO_4, and concentrated under reduced pressure. The crude residue was subjected to column chromatography (n-hexane:AcOEt = 4:1∼3:1) to give ^{t}butyl 5-benzyloxy-1-[1-(4-chlorophenyl)-3-phenyl-propyl]-2-methyl indole 3-acetate (337 mg, 51%) as a yellow oil. To a solution of the obtained compound (44.0 mg, 0.0758 mmol) in CH_2Cl_2 (1.50 mL) was added CH_3COOH (0.400 mL) dropwise, and the mixture was stirred for 3 h. The solvent was removed, and the solid was subjected to column chromatography (CH_2Cl_2:MeOH = 20:1) to give **30** (15.0 mg, 38%) as a dark yellow oil: ^{1}H NMR (300 MHz, $CDCl_3$) δ (ppm) 7.40−6.84 (16H, m), 6.68 (1H, dd, J = 8.9 Hz, 2.6 Hz), 5.34 (1H, d, J = 8.0 Hz), 5.00 (2H, s), 3.64 (2H, s), 2.69−2.64 (2H, m), 2.34 (2H, t, J = 7.5 Hz), 2.07 (3H, s); LRMS (EI) m/z 523 (M^+). HRMS (EI) calcd for $C_{33}H_{30}NO_3Cl$, 523.1914; found, 523.1900.

Succinic Acid Benzyl Ester 3-Carboxymethyl-1-[1-(4-chlorophenyl)-3-phenyl-propyl]-2-methyl Indol-5-yl Ester (31). To a solution of **33** (400 mg, 1.14 mmol) and ^{t}BuOK (154 mg, 1.37 mmol) in DMF (7.00 mL) was added a solution of p-$ClC_6H_4CHBrCH_2CH_2Ph$ in DMF (1.00 mL), and the mixture was stirred at room temperature for 14 h. To the mixture was added H_2O. The organic compound was extracted with AcOEt, washed with brine, dried over Na_2SO_4, and concentrated under reduced pressure. The crude residue was subjected to column chromatography (n-hexane:AcOEt = 4:1∼3:1) to give ^{t}butyl 5-benzyloxy-1-[1-(4-chlorophenyl)-3-phenyl-propyl]-2-methyl indole 3-acetate (337 mg, 51%) as a yellow oil. To a solution of the obtained compound (337 mg, 0.581 mmol) in acetic acid (2.00 mL) and AcOEt (10.0 mL) was added Pd-C (170 mg) under H_2 (3.80 atm), and the mixture was stirred at room temperature for 4.5 h. The mixture was filtered, and solvent was removed. The residue was subjected to column chromatography (n-hexane:AcOEt = 4:1∼3:1) to give ^{t}butyl 1-[1-(4-chloro-phenyl)-3-phenyl-propyl]-5-hydroxy-2-methyl indole 3-acetate (185 mg, 65%) as a white powder. To a solution of the obtained compound (183 mg, 0.373 mmol) in CH_2Cl_2 (6.00 mL) was added succinic acid monobenzyl ester (85.0 mg, 0.410 mmol), DCC (115 mg, 0.560 mmol), and DMAP (4.50 mg, 0.0373 mmol), and the mixture was stirred for 12 h. The mixture was filtered, and the solvent was removed. The crude residue was subjected to column chromatography (n-hexane:AcOEt = 3:1) to give succinic acid benzyl ester 3-^{t}butoxycarbonylmethyl-1-[1-(4-chloro-phenyl)-3-phenyl-propyl]-2-methyl-1H-indole-5-yl ester (249 mg, 98%) as a pale yellow oil. The compound (249 mg, 0.366 mmol) and Celite 535 (44.0 mg) were stirred at 180−190 °C for 8 h. The crude residue was subjected to column chromatography (CH_2Cl_2:MeOH = 20:1) to give **31** (150 mg, 66%) as a yellow oil: ^{1}H NMR (270 MHz, $CDCl_3$) δ (ppm) 7.33−6.96 (16H, m), 6.70 (1H, dd, J = 6.8 Hz, 2.2 Hz), 5.43 (1H, m), 5.13 (2H, s), 3.67 (2H, s), 2.88−2.76 (6H, m), 2.42 (2H,m), 2.13 (3H, s); LRMS (EI) m/z 623 (M^+). HRMS (EI) calcd for $C_{37}H_{34}NO_6Cl$, 623.2074; found, 623.2054.

Succinic Acid Benzyl Ester 3-Carboxymethyl-1-[1-(4-chlorophenyl)-4-phenyl-butyl]-2-methyl Indol-5-yl Ester (32). To a solution of **33** (155 mg, 0.441 mmol) and ^{t}BuOK (59.0 mg, 0.529 mmol) in DMF (2.00 mL) was added a solution of p-$ClC_6H_4CHBrCH_2CH_2OPh$ (180 mg, 0.529 mmol) in DMF (1.50 mL), and the mixture was stirred for 12 h. To the mixture was added H_2O, and the organic compound was extracted with AcOEt, washed with aqueous NaCl, dried over Na_2SO_4, filtered, and concentrated. The crude residue was subjected to column chromatography (n-hexane:AcOEt = 4:1) to give N-alkylated compound (96.0 mg, 36%) as a yellow oil. To a solution of N-alkylated compound (96.0 mg, 0.157 mmol) in AcOEt (3.00 mL) and AcOH (0.600 mL) was added Pd/C (46.0 mg) under H_2 (3.00 atm), and the mixture was stirred for 5 h. The mixture was filtered, and solvent was removed. The crude residue was subjected to column chromatography (n-hexane:AcOEt = 3:1) to give ^{t}butyl-[1-(4-chloro-phenyl)-4-phenoxy-butyl]-5-hydroxy-2-methyl indole-3-acetate (50.0 mg, 61.1%) as a pale yellow powder. To a solution of the resulting compound (50.0 mg, 0.0961 mmol) in CH_2Cl_2 (1.60 mL) were added succinic acid monobenzyl ester (23.0 mg, 0.106 mmol), DCC (31.0 mg, 0.144 mmol), and DMAP (1.20 mg, 0.00961 mmol), and the mixture was stirred for 12 h. The mixture was filtered, and the organic compound was washed with water and brine, dried over Na_2SO_4, filtered, and concentrated. The crude residue was subjected to column chromatography (n-hexane:AcOEt = 3:1) to give succinic acid benzyl ester 3-^{t}butoxycarbonyl-methyl-1-[1-(4-chloro-phenyl)-4-phenoxy-butyl]-2-methyl-1H-indole-5-yl ester (62.0 mg, 91%) as a colorless oil. To a solution of the obtained compound (41.0 mg, 0.0577 mmol) in CH_2Cl_2 (1.30 mL) was added CF_3COOH (0.300 mL), and the mixture was stirred for 12 h. The solvent was removed, and the crude residue was subjected to preparative TLC (AcOEt:MeOH = 20:1) to give **32** (18.9 mg, 50%) as a yellow oil: ^{1}H NMR (300 MHz, $CDCl_3$) δ (ppm) 7.28−6.74 (16H, m), 6.62 (1H, dd, J = 8.9 Hz, 2.3 Hz), 5.49 (1H, dd, J = 11.1 Hz, 4.8 Hz), 5.08 (2H, s), 3.87−3.73 (2H, m), 3.60 (2H, s), 2.85−2.45 (6H, m), 2.26 (3H,s), 1.70−1.30 (2H, m); LRMS (FAB) m/z 676 (M^+ + Na); HRMS (FAB) calcd for $C_{38}H_{36}NO_7ClNa$, 676.2078; found, 676.2057.

Enzyme Inhibition. AR was partially purified from bovine lenses according to the method of Kinoshita et al.[45] The in vitro

inhibitory activity of test compounds was determined using D,L-glyceraldehyde as a substrate. The test compound was dissolved in dimethyl sulfoxide (DMSO) at the desired concentration. The assay was performed in a reaction mixture of 5 mL of 60 mM sodium phosphate buffer (pH 6.2) which contained the enzyme, 0.13 mM (0.5 mg) NADPH, and 1.5 mM (0.68 mg) D,L-glyceraldehyde. The enzyme activity was measured by the decrease in the oxidation ratio of NADPH in 30 min by monitoring the absorbance at 340 nm at 25 °C with a Hitachi U-1080 photometer. The test compounds were initially assayed for their inhibition of AR at a concentration of 15 or 5 μg/mL. If an inhibition of more than 40% was observed at a concentration of 15 μg/mL, the compound was classified as active. Those that exhibited >50% inhibition at the initial concentration were tested at several concentrations to obtain their IC_{50} values.

Acknowledgment. This work was performed through Special Coordination Funds for Promoting Science and Technology of the Science and Technology Agency of the Japanese Government.

References

(1) Kodor, P. F. The role of aldose reductase in the development of diabetic complications. *Med. Res. Rev*. **1988**, *8*, 325−352.
(2) Tomlinson, D. R.; Stevens, E. J.; Diemel, L. T. Aldose reductase inhibitors and their potential for the treatment of diabetic complications. *Trends Pharmacol. Sci*. **1994**, *15*, 293−297.
(3) Costantino, L.; Rastelli, G.; Vianello, P.; Cignarella, G.; Barlocco, D. Diabetes complications and their potential prevention: aldose reductase inhibition and other approaches. *Med. Res. Rev*. **1999**, *19*, 3−23.
(4) Carper, D.; Wistow, G.; Nishimura, C.; Graham, C.; Watanabe, K.; Fuji, Y.; Hayaishi, H.; Hayaishi, O. A superfamily of NADPH-dependent reductases in eukaryotes. *Exp. Eye Res*. **1988**, *49*, 377−388.
(5) Mylari, B. L.; Larson, E. R.; Beyer, T. A.; Zembrowski, W. J.; Aldinger, C. E.; Dee, M. F.; Siegel, T. W.; Singleton, D. H. Novel, potent aldose reductase inhibitors: 3,4-dihydro-4-oxo-3-[[5-(trifluoromethyl)-2-benzothiazoyl]methyl]-1-phthalazineacetic acid (zopolrestat) and congeners. *J. Med. Chem*. **1991**, *34*, 108−122.
(6) Wrobel, J.; Millen, J.; Sredy, J.; Dietrich, A.; Gorham, B. J.; Malamas, M.; Kelly, J. M.; Bauman, J. G.; Harrison, M. C.; Jones, L. R.; Guinosso, C.; Sestanj, K. Synthesis of tolrestat analogues containing additional substituents in the ring and their evaluation as aldose inhibitors. Identification of potent, orally active 2-fluoro derivatives. *J. Med. Chem*. **1991**, *34*, 2504−2520.
(7) Yamagishi, M.; Yamada, Y.; Ozaki, K.; Asao, M.; Shimizu, R.; Suzuki, M.; Matsumoto, M.; Matsuoka, Y.; Matsumoto, K. Biological activities and quantitative structure−activity relationships of spiro[imidazolidine-4,4′(1′*H*)-quinazoline]-2,2′,5-(3′*H*)-triones as aldose reductase inhibitors. *J. Med. Chem*. **1992**, *35*, 2085−2094.
(8) Kawamura, M.; Hamanaka, N. Development of Eparlestat (Kinedak), aldose reductase inhibitor. *J. Synth. Org. Chem*. **1997**, *37*, 787−792.
(9) Wilson, D. K.; Bohren, K. M.; Gabbay, K. H.; Quiocho, F. A. An unlikely sugar substrate site in the 1.65 Å structure of the human aldose reductase holoenzyme implicated in diabetic complications. *Science* **1992**, *257*, 81−84.
(10) Harrison, D. H.; Bohren, K. M.; Ringe, D.; Petsko, G. A.; Gabbay, K. H. An anion binding site in human aldose reductase: mechanistic implications for the binding of citrate, cacodylate, and glucose 6-phosphate. *Biochemistry* **1994**, *33*, 2011−2020.
(11) Bohren, K. M.; Grimshaw, C. E.; Lai, C. J.; Harrison, D. H.; Ringe, D.; Petsko, G. A.; Gabbay, K. H. Tyrosin-48 is the proton donor and histidine-110 directs substrate stereochemical selectivity in the reduction reaction of human aldose reductase: enzyme kinetics and crystal structure of the Y48H mutant enzyme. *Biochemistry* **1994**, *33*, 2021−2032.
(12) Várnai, P.; Warshel, A. Computer simulation studies of the catalytic mechanism of human aldose reductase. *J. Am. Chem. Soc*. **2000**, *122*, 3849−3860.
(13) Lee Y. S.; Hodoscek M.; Brooks. B. R.; Kador P. F. Catalytic mechanism of aldose reductase studied by the combined potentials of quantum mechanics and molecular mechanics. *Biophys. Chem*. **1998**, *70*, 203−16.
(14) Costantino, L.; Rastelli, G.; Vescovini, K.; Cignarella, G.; Vianello, P.; Del Corso, A.; Cappiello, M.; Mura, U.; Barlocco, D. Synthesis, activity, and molecular modeling of a new series of tricyclic pyridazinones as selective aldose reductase inhibitors. *J. Med. Chem*. **1996**, *39*, 4396−4405.
(15) *Structure-Based Drug Design*; Veerapandian P., Ed.; Marcel Dekker Inc.: New York, 1997.
(16) Hicks, S.; Assefa, H.; Sindelar, R. Computer-aided design of enzyme inhibitors: recent studies. *Curr. Opin. Drug Discovery Dev*. **1998**, *1*, 223−234.
(17) Lam, P. Y. S.; Jadhav, P. K.; Eyermann, C. J.; Hodge, C. N.; Ru, Y.; Bacheler, L. T.; Meek, J. L.; Otto, M. J.; Rayner, M. M.; Wong, Y. N.; Chang, C.-H.; Weber, P. C.; Jackson, D. A.; Sharpe, T. R.; Erickson-Viitanen, S. Rational design of potent, bioavailable, nonpeptide cyclic Ureas as HIV protease inhibitors. *Science* **1994**, *263*, 380−384.
(18) Nicklaus, M. C.; Pommier, Y. HIV-1 integrase pharmacophore: discovery of inhibitors through three-dimensional database searching. *J. Med. Chem*. **1997**, *40*, 920−929.
(19) Verlinde, C. L. M. J.; Hol, W. G. J. Structure-based drug design: progress, results and challenges. *Structure* **1994**, *2*, 577−587.
(20) Kuntz, I. D. Structure-based strategies for drug design and discovery. *Science* **1992**, *257*, 1078−1082.
(21) Sarmiento, M.; Wu, L.; Keng, Y.-F.; Song, L.; Luo, Z.; Huang, Z.; Wu, G.-Z.; Yuan, A. K.; Zhang, Z.-Y. Structure-based discovery of small molecule inhibitors targeted to protein tyrosine phosphatase 1B. *J. Med. Chem*. **2000**, *43*, 146−155.
(22) Perola, E.; Xu, K.; Kollmeyer, T. M.; Kaufmann, S. H.; Prendergast, F. G.; Pang, Y.-P. Successful virtual screening of a chemical database for farnesyltransferase inhibitor leads. *J. Med. Chem*. **2000**, *43*, 401−408.
(23) Mizutani, M. Y.; Tomioka, N.; Itai, A. Rational automatic search method for stable docking models of protein and ligand. *J. Mol. Biol*. **1994**, *243*, 310−326.
(24) Lee Y. S.; Chen, Z.; Kador P. F. Molecular modeling studies of the binding modes of aldose reductase inhibitors at the active site of human aldose reductase. *Bioorg. Med. Chem*. **1998**, *6*, 1811−1819.
(25) Rastelli, G.; Vianello, P.; Barlocco, D.; Costantino, L.; Corso, A. D.; Mura, U. Structure-based design of an inhibitor modeled at the substrate active of aldose reductase. *Bioorg. Med. Chem. Lett*. **1997**, *7*, 1897−1902.
(26) Wilson, D. K.; Quiocho, F. A.; Petrash, J. M. Structural studies of aldose reductase inhibition. In *Structure-Based Drug Design*; Veerapandian P., Ed.; Marcel Dekker Inc.: New York, 1997; pp 229−246.
(27) Shen, C.; Sigman, D. S. New inhibitors of aldose reductase: antioximes of aromatic aldehydes. *Arch. Biochem. Biophys*. **1991**, *286*, 596−603.
(28) Berman, H. M.; Westbrook, J.; Feng, Z.; Gilliland, G.; Bhat, T. N.; Weissig, H.; Shindyalov, I. N.; Bourne, P. E. The protein data bank. *Nucleic Acids Res*. **2000**, *28*, 235−242.
(29) Iwata, Y.; Kasuya, A.; Miyamoto S. A method for assessing the side chain orientations of histidine, asparagine, and glutamine as well as the protonation forms of histidine in protein structures. *Drug Des. Discovery*, in press.
(30) Sugiyama, K.; Chen, Z.; Lee, Y. S.; Kador, P. F. Isolation of a noncovalent aldose reductase-nucleotide-inhibitor complex. *Biochem. Pharmacol*. **2000**, *59*, 329−36.
(31) Harrison, D. H.; Bohren, K. M.; Petsko, G. A.; Ringe, D.; Gabbay, K. H. The alrestatin double-decker: binding of two inhibitor molecules to human aldose reductase reveals a new specificity determinant. *Biochemistry* **1997**, *36*, 16134−40.
(32) Nakano T.; Petrash, J. M. Kinetic and spectroscopic evidence for active site inhibition of human aldose reductase. *Biochemistry* **1996**, *35*, 11196−11202.
(33) Pearlman, D. A.; Case, D. A.; Caldwell, J.; Seibel, G.; Singh, U. C.; Weiner, P.; Kollman, P. A. AMBER 4.0; University of California: San Francisco, 1990.
(34) Version 4.1.1. Wavefunction, Inc.: Irvine, CA, 1993 (http://www.wavefun.com).
(35) Brooks, B. R.; Bruccoleri, R. E.; Olafson, B. D.; States, D. J.; Swaminathan, S.; Karplus, M. CHARMM: a program for macromolecular energy, minimization, and dynamics calculations. *J. Comput. Chem*. **1983**, *4*, 187−217.
(36) QUANTA version 97/CHARMm version 23; Molecular Simulations, Inc.: San Diego (http://www.msi.com).
(37) Molecular Design Limited Information Systems, San Leandro, CA (http://www.mdl.com).
(38) Tomioka, N.; Itai, A. GREEN: A program package for docking studies in rational drug design. *J. Comput.-Aided Mol. Des*. **1994**, *8*, 347−366.
(39) Wang, S.; Zaharevitz, D. W.; Sharma, R.; Marquez, V. E.; Lewin, N. E.; Du, L.; Blumberg, P. M.; Milne, G. W. A. The discovery of novel, structurally diverse protein kinase C agonists through computer 3D-database pharmacophore search. Molecular Modeling studies. *J. Med. Chem*. **1994**, *37*, 4479−4489.

(40) Verlinde, C. L. M. J.; Kim, H.; Bernstein, B. E.; Mande, S. C.; Hol, W. G. J. Antitrypanosomiasis drug development based on structures of glycolytic enzymes. In *Structure-Based Drug Design*; Veerapandian P., Ed.; Marcel Dekker Inc.: New York, 1997; pp 365−394.

(41) Muegge, I.; Martin, Y. C. A general and fast scoring function for protein−ligand interactions: a simplified potential approach. *J. Med. Chem*. **1999**, *42*, 791−804.

(42) Urzhumtsev, A.; Tête-Favier, F.; Mitschler, A.; Barbanton, J.; Barth, P.; Urzhumtseva, L.; Biellmann, J.-F.; Podjarny, A. D.; Moras, D. A 'specificity' pocket inferred from the crystal structures of the complexes of aldose reductase with the pharmaceutically important inhibitors tolrestat and sorbinil. *Structure* **1997**, *5*, 601−612.

(43) Wilson, D. K.; Tarle, I.; Petrash J. M.; Quiocho, F. A. Refined 1.8 Å structure of human aldose reductase complexed with the potent inhibitor zopolrestat. *Proc. Natl. Acad. Sci. U.S.A.* **1993**, *90*, 9847−9851.

(44) Costantino, L.; Rastelli, G.; Gamberini, M. C.; Giovannoni, M. P.; Piaz, V. D.; Vianello, P.; Barlocco, D. Isoxazolo-[3,4-*d*]-pyridazin-7-(6*H*)-ones as a potential substrate for new aldose reductase inhibitors. *J. Med. Chem*. **1999**, *42*, 1894−1900.

(45) Hayman, S.; Kinoshita, J. H. Isolation and properties of lens aldose reductase. *J. Biol. Chem*. **1965**, *240*, 877−882.

JM000483H